Multimodal Feature Learning and Interpretable Feature Selection for Elevator Fault Diagnosis

Haokun Wu[1], Qiwei Tang[2] and Wang Zhang[3]

***Abstract*— Modern intelligent building systems require reliable vertical transportation solutions. Equipment malfunctions in elevator systems can significantly impact operational safety and passenger experience. Developing efficient diagnosis approaches becomes crucial for minimizing service interruptions. Current condition monitoring techniques, primarily designed for gear systems, require substantial adaptation for elevator-specific applications. This research proposes an integrated feature learning framework combining multidomain signal analysis with interpretable machine learning. Our methodology extracts temporal characteristics, spectral energy distributions, and system-specific frequency components from triaxial vibration data. These multimodal features feed into a kernel-based classifier for condition classification. To enhance model interpretability and efficiency, we employ cooperative game theory for feature importance analysis. Experimental validation demonstrates three key advantages: (1) Triaxial signal processing captures spatial-temporal patterns more effectively than single-axis approaches, improving diagnosis precision by 3.2-5.7% across test cases. (2) Incorporating domain-specific frequency signatures boosts classification accuracy by 4.1% compared to generic feature sets. (3) Our feature selection mechanism reduces dimensionality by 60-95% while maintaining 96.7% mean accuracy, significantly lowering computational overhead.**

I. INTRODUCTION

Contemporary urban infrastructure increasingly relies on intelligent building ecosystems that incorporate advanced automation and data analytics for enhanced operational management, improving energy utilization, user experience, security, and resource management [1]. Vertical transportation, including modern elevators with intelligent functionalities, plays a critical role, using real-time monitoring and predictive analytics to streamline operations, minimize wait times, and reduce energy consumption [2], [3].

Elevator system failures disrupt operations and pose safety risks [4]. Modern diagnosis, via integrated sensor networks, continuously monitor operational parameters and initiate automated analysis to predict failures, improving system reliability and safety.

Elevator fault detection faces challenges, as traditional maintenance follows predetermined schedules without considering actual system conditions [5]. Vibration analysis provides valuable insights into system health [6], but current diagnosis rely on technician expertise and empirical methods, leading to inconsistent results [7].

The integration of IoT [8] and machine learning [9] transforms diagnosis by enabling comprehensive data collection and pattern recognition. Methods such as neural networks [10], support vector machines [11], and probabilistic graphical models [12] are commonly used.

Recent systems, like the Smart Bearing Diagnosis System (SBDS) [13], combine convolutional feature extraction with neuro-fuzzy classification, while deep learning [14] and autoencoders [15] are used for elevator-specific diagnosis . However, data imbalance and limited fault samples challenge these methods' effectiveness.

Signal processing techniques, such as wavelet packet analysis [16] and frequency domain feature extraction [17], show promise in overcoming these limitations. Methods for non-stationary vibration signals, including decomposition [18] and dimensionless feature extraction [19], are also explored.

A key limitation of current methods is their adaptation from bearing diagnosis to elevators, as the complex mechanical architecture requires specialized approaches. Increasing feature dimensionality can improve accuracy but often reduces model generalization [20], extends training durations, and increases computational overhead [21]. A balance between feature richness and model complexity is essential for effective fault diagnosis.

Our research addresses these challenges through a comprehensive approach that combines structural analysis with advanced signal processing. The methodology focuses on extracting system-specific frequency characteristics from vibration patterns, complemented by support vector machine classification. To optimize feature utilization, we implement SHapley Additive exPlanations (SHAP) [22] for feature selection [23], yielding several significant contributions:

- Triaxial signal processing preserves comprehensive spatial-temporal information, enhancing practical applicability compared to traditional uniaxial approaches.
- Incorporation of system-specific frequency characteristics improves diagnosis accuracy while maintaining adaptability across different elevator configurations.
- Strategic feature selection through SHAP analysis reduces computational requirements without compromising accuracy, effectively addressing high-dimensionality challenges and minimizing overfitting risks.

*This research was funded by the Science and Technology Fund, FDCT, Macau SAR, under grant 0101/2022/A.

[1]Institute of Systems Engineering, Macau University of Science and Technology, Taipa, Macau SAR, China 3220005901@student.must.edu.mo

[2]Hitachi Building Technology (Guangzhou) Co., Ltd., Guangzhou, China tangqiwei@hitachi-helc.com

[3]The Third Surveying and Mapping Institute of Hunan Province, Changsha, China zwfzyj822@163.com

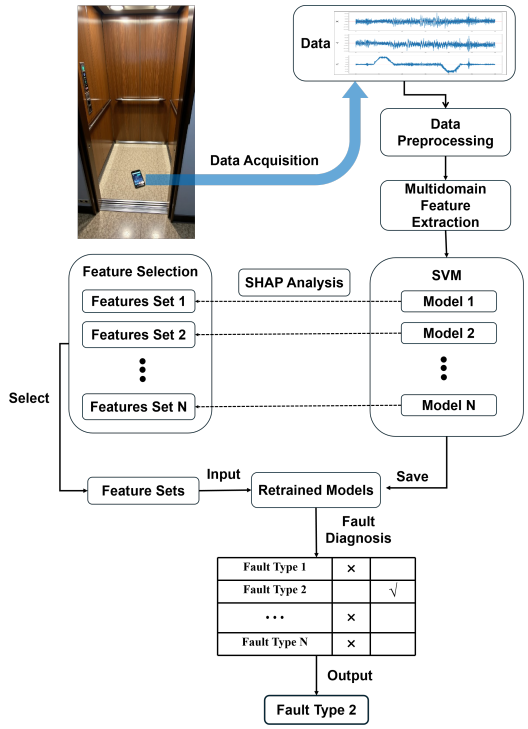

Fig. 1: Fault diagnosis model

II. Methodology

A. Proposed Framework for Fault Diagnosis

The architecture of the elevator fault diagnosis system is illustrated in Fig. 1. The workflow is divided into several phases: feature extraction, feature selection, model training and refinement, followed by fault diagnosis. The steps are as follows:

Initially, real-time multi-dimensional data from the elevator is collected via a mobile device. The raw data undergoes preprocessing, including cleaning and normalization, to prepare it for feature extraction. During feature extraction, important features are derived based on key operational parameters such as maximum speed, suspension ratio, and car pulley dimensions.

The extracted features are subsequently fed into the SVM model for initial training, producing a set of preliminary fault classification models, denoted as Model M_1 through Model M_N. Feature selection is performed using SHAP (SHapley Additive exPlanations), which assesses the contribution of each feature to the model's predictions, helping to remove redundant or irrelevant features. The model is retrained using the refined feature set, improving fault detection accuracy. The retrained model is saved for future use in fault diagnosis.

Finally, during the fault diagnosis phase, the system continuously monitors real-time elevator data, extracts features, and feeds them into the retrained SVM model. The model then classifies the data and provides the specific fault diagnosis of the elevator.

B. Data Acquisition Pipeline

1) Smartphone-based Sensing: In our study, the elevator vibration data is captured using an Honor 60 smartphone, as opposed to a typical IoT edge device. This phone is equipped with an inbuilt triaxial accelerometer that operates at a sampling rate of 500 Hz. The accelerometer is placed at the center of the elevator cabin floor. The data collected consists of triaxial vibration signals along the X, Y, and Z axes. Specifically, the X-axis is oriented perpendicular to the elevator door, the Y-axis is parallel to the door, and the Z-axis is vertical, perpendicular to the floor.

2) Data Preprocessing: Prior to feature extraction, several preprocessing steps are undertaken to enhance data quality and ensure its suitability for analysis.

(1) Data Cleaning

To guarantee that the dataset used for training is comprehensive and encompasses all necessary features, incomplete samples are discarded, as depicted in Figure 2. A valid sample must represent a full operational cycle of the elevator, which includes phases such as idle, acceleration, constant speed, deceleration, and halting.

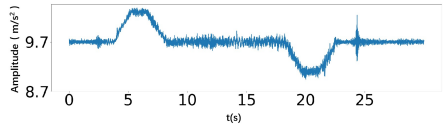

(a) Complete sample.

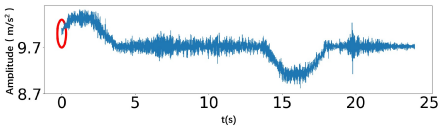

(b) Incomplete sample.

Fig. 2: Z-axis vibration data for both complete and incomplete samples.

(2) Segmentation of Operational Stages

The elevators vibration characteristics vary between the acceleration, deceleration, and constant velocity phases. As such, each phase necessitates distinct feature extraction. To facilitate efficient feature extraction in subsequent steps, the elevators entire operational cycle is partitioned into three stages: acceleration, constant velocity, and deceleration.

C. Feature Extraction Across Multiple Domains

1) Features in the Time Domain: Define the vibration signal as $x = \{x_1, x_2, \ldots, x_n\}$. Table I displays the time-domain features for the X, Y, and Z axes across the different operational stages of the elevator. In Table I, μ_x represents the mean value of x.

TABLE I: Mathematical Expressions of Time Domain Features

Feature	Expression
Variance	$\frac{1}{n}\sum_{i=1}^{n}(x_i-\mu_x)^2$
Peak-to-peak Range	$\max(x)-\min(x)$
Root Mean Square(RMS)	$\sqrt{\frac{1}{n}\sum_{i=1}^{n}x_i^2}$
Kurtosis	$\frac{\frac{1}{n}\sum_{i=1}^{n}(x_i-\mu_x)^4}{\left(\sqrt{\frac{1}{n}\sum_{i=1}^{n}(x_i-\mu_x)^2}\right)^4}$
Skewness	$\frac{\frac{1}{n}\sum_{i=1}^{n}(x_i-\mu_x)^3}{\left(\sqrt{\frac{1}{n}\sum_{i=1}^{n}(x_i-\mu_x)^2}\right)^3}$
Crest Factor	$\frac{\max\lvert x\rvert}{\sqrt{\frac{1}{n}\sum_{i=1}^{n}(x_i-\mu_x)^2}}$
Shape Factor	$\frac{\text{RMS}}{\frac{1}{n}\sum_{i=1}^{n}\lvert x_i\rvert}$
Margin Factor	$\frac{\max\lvert x\rvert}{\left(\frac{1}{n}\sum_{i=1}^{n}\sqrt{\lvert x_i\rvert}\right)^2}$
Impulse Factor	$\frac{\max\lvert x\rvert}{\frac{1}{n}\sum_{i=1}^{n}\lvert x_i\rvert}$

2) Frequency Features of the Elevator: To account for the unique design and operational properties of the elevator system, we define its frequency characteristics. The main components of interest are the traction wheel, traction motor, guide wheel, car pulley, and rope strands. The corresponding frequencies are as follows:

(1) Traction wheel rotational frequency (f_s):

$$f_s = \frac{V \cdot I}{\pi \cdot D_s}, \tag{1}$$

where V is the velocity, I represents the hanging ratio, and D_s is the diameter of the traction wheel.

(2) Traction motor pulse frequency (f_m):

$$f_m = \frac{f_s \cdot P}{2}, \tag{2}$$

where P being the number of poles in the motor.

(3) Guide wheel rotational frequency (f_{bp}):

$$f_{bp} = \frac{V \cdot I}{\pi \cdot D_{bp}}, \tag{3}$$

where D_{bp} denotes the guide wheels diameter.

(4) Car pulley rotational frequency (f_{cp}):

$$f_{cp} = \frac{V \cdot I}{\pi \cdot D_{cp}}, \tag{4}$$

where D_{cp} representing the diameter of the car pulley.

(5) Rope strand frequency (f_{rp}):

$$f_{rp} = \frac{V}{pr}, \tag{5}$$

where pr is the spacing between the strands of the rope.

During the analysis of elevator fault vibrations, it is observed that multiples of these frequencies (such as two and three times the base frequencies) are also relevant fault indicators. As shown in Fig. 3, we also consider these frequency multipliers as part of the fault features.

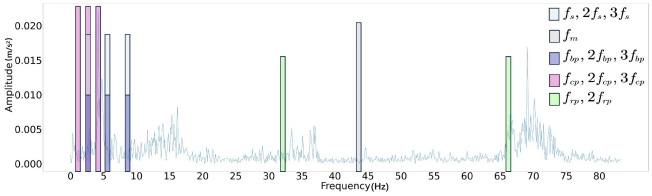

Fig. 3: Elevator frequency bands for feature extraction.

3) Wavelet Packet Energy: Wavelet Packet Decomposition (WPD) breaks down the original vibration signal into multiple packets, with the energy of each packet serving as a feature of the signal [24]. After applying the decomposition, eight packets are generated at the third layer, labeled as P_j^3, where $j = 0, 1, 2, 3, 4, 5, 6, 7$. The energy corresponding to each packet is computed as:

$$E_{3j} = \sum\nolimits_{i=1}^{N}(x_{ij})^2, \tag{6}$$

where i serves as the index for the data points, where j represents the packet number, where N is the data length, where x_{ij} denotes the amplitude of the discrete points in packet P_j^3. The total energy, E_3, for the entire signal is the sum of the energies from all packets:

$$E_3 = \sum\nolimits_{j=0}^{7} E_{3j}. \tag{7}$$

Following the normalization of the energies, the frequency-domain feature vector $\boldsymbol{X_f}$ for the original vibration signal is derived:

$$\boldsymbol{X_f} = \frac{[E_{30}, E_{31}, E_{32}, E_{33}, E_{34}, E_{35}, E_{36}, E_{37}]}{E_3}. \tag{8}$$

A total of 165 features are calculated during the feature extraction process. Among these, 81 time-domain features are derived from the triaxial vibration data, considering the acceleration, deceleration, and constant velocity phases, as shown in Table I. Additionally, the frequencies and their multiples for the elevator model are calculated using (1) through (5). Based on these frequency values, 12 frequency-based features are extracted. Wavelet packet energy values are also computed for each axis at every operational stage, following the equations (6) to (8), yielding a total of 72 features.

Normalizing these features accelerates the gradient descent process, promoting faster convergence during the training of the network. The SVM classifier utilizes the normalized feature set as input during the fault diagnosis phase.

D. Support Vector Machine

The Support Vector Machine (SVM) constructs a classification model by mapping non-linear data into a higher-dimensional space, facilitating the identification of a hyperplane that separates different classes. The SVM algorithm employs a nonlinear transformation function $\psi(\mathbf{z})$ to project the input data $\mathbf{z}$ onto this high-dimensional feature space, enabling the application of linear techniques to model the

decision function. The classifier plane equation is formulated as:

$$\mathbf{w} \cdot \psi(\mathbf{z}) + b = 0, \tag{9}$$

where $\mathbf{w}$ represents the weight vector defining the orientation and direction of the hyperplane, $\psi(\mathbf{z})$ is the feature transformation function mapping the input data into a higher-dimensional space, and b is the bias term shifting the hyperplane from the origin. The symbol $\cdot$ denotes the dot product operation.

The decision function, which classifies new data points, is given by:

$$g(\mathbf{z}) = \text{sign}(\mathbf{w} \cdot \psi(\mathbf{z}) + b). \tag{10}$$

This approach enables the linear classifier to handle nonlinear problems effectively.

To address nonlinearity, the optimization problem for determining the classification hyperplane is expressed as:

$$\begin{aligned} \min_{\beta} \quad & \frac{1}{2}\mathbf{w}^T\mathbf{w} - D\sum\nolimits_{k=1}^{m} \zeta_k, \\ \text{s.t.} \quad & \upsilon_k(\mathbf{w}^T \cdot \mathbf{z}_k + b) \geq 1 - \zeta_k, \end{aligned} \tag{11}$$

where $\zeta_k \geq 0$ for $k = 1, 2, \ldots, m$, D is a regularization parameter balancing margin width and misclassification tolerance, and ζ_k are slack variables representing margin violations. By introducing the Lagrangian function, the optimization problem is transformed into its dual form:

$$\begin{aligned} \min_{\beta} \quad & \frac{1}{2}\sum\nolimits_{k=1}^{m}\sum\nolimits_{l=1}^{m} \upsilon_k\upsilon_l\beta_k\beta_l\Gamma(\mathbf{z}_k, \mathbf{z}_l) - \sum\nolimits_{k=1}^{m}\beta_k, \\ \text{s.t.} \quad & \sum\nolimits_{k=1}^{m}\beta_k\upsilon_k = 0, \quad 0 \leq \beta_k \leq D, \quad k = 1, 2, \ldots, m, \end{aligned} \tag{12}$$

where β_k is the Lagrange multiplier associated with each training sample, and υ_k and υ_l are the class labels. If $0 \leq \beta_k \leq D$, the data point $\mathbf{z}_k$ is considered a support vector. The kernel function $\Gamma(\mathbf{z}_k, \mathbf{z}_l)$ is defined as:

$$\Gamma(\mathbf{z}_k, \mathbf{z}_l) = \psi(\mathbf{z}_k) \cdot \psi(\mathbf{z}_l). \tag{13}$$

E. SHapley Additive exPlanations

SHAP is a widely utilized technique for interpreting model outputs by clarifying how each input feature contributes to a given prediction. It is grounded in cooperative game theory, specifically the Shapley value.

1) Shapley Value: Originating from cooperative game theory [25], the Shapley value quantifies the individual contribution of each feature to the final model prediction. It is computed by averaging the marginal contribution of a feature over all possible subsets of the remaining features. The Shapley value φ_j for the j-th feature is expressed as:

$$\varphi_j = \sum_{\mathcal{S}\subseteq\mathcal{M}\setminus\{j\}} \frac{|\mathcal{S}|! \cdot (m - |\mathcal{S}| - 1)!}{m!} \left[g(\mathcal{S} \cup \{j\}) - g(\mathcal{S})\right], \tag{14}$$

where m is the total number of input features, $\mathcal{M}$ represents the set of all features, and $\mathcal{S}$ is a subset of features excluding the j-th feature. The function $g(\cdot)$ denotes the models predicted outcome for a given feature subset.

For illustration, consider a model with three features ($m = 3$) where we calculate the Shapley value for feature $j = 1$. The possible subsets $\mathcal{S}$ are $\emptyset$, $\{2\}$, and $\{3\}$. Assuming model predictions $g(\emptyset) = 0.2$, $g(\{1\}) = 0.7$, $g(\{1, 2\}) = 0.9$, and $g(\{1, 3\}) = 0.8$, the Shapley value φ_1 is computed as:

$$\begin{aligned} \varphi_1 &= \frac{0! \cdot 2!}{3!}(0.7 - 0.2) + \frac{1! \cdot 1!}{3!}(0.9 - 0.2) \\ &\quad + \frac{1! \cdot 1!}{3!}(0.8 - 0.2) \\ &= \frac{2}{6}(0.5) + \frac{1}{6}(0.7) + \frac{1}{6}(0.6) \\ &= 0.48. \end{aligned} \tag{15}$$

This demonstrates how the Shapley value aggregates weighted marginal contributions across all feature combinations.

2) Local Interpretable Model-agnostic Explanations: Ribeiro *et al.* proposed Local Interpretable Model-agnostic Explanations (LIME) to elucidate individual model predictions by constructing local approximations near the prediction point [26]. This method is particularly valuable for intricate or opaque models, aiming to deliver straightforward and comprehensible interpretations even for highly complex systems.

LIME employs the concept of "interpretable inputs," which are simplified versions of the original input features, represented as $\mathbf{z}'$. The mapping function $\mathbf{z} = h_z(\mathbf{z}')$ converts these binary vectors back into the original feature space, with the transformation h_z varying according to the nature of the input space.

To compute the Shapley value φ, LIME seeks to minimize the following objective function:

$$\zeta = \arg\min_{q\in\mathcal{Q}} J(g, q, \pi_{z'}) + \Lambda(q), \tag{16}$$

where g represents the original predictive model, and q is the locally fitted approximation model. The term $J(g, q, \pi_{z'})$ denotes the loss function, which quantifies the divergence between the predictions of the original and local models, weighted by the local kernel $\pi_{z'}$. The function $\Lambda(q)$ imposes a regularization penalty on the complexity of q, ensuring that the weights in the linear approximation correspond to the Shapley values φ.

III. EXPERIMENTS

A. Simulation of Elevator Faults

In this study, five distinct types of faults are simulated on an experimental six-floor elevator system. These faults include unbalanced loads, uneven rail joints, uneven rope tension, surface wear of the guide shoe, and uneven surfaces in the car pulley rope groove.

TABLE II: Results of Accuracy Verification Experiments.

Fault	Fault data	Accuracy	F1 Score
UL	101	93.33%	94.87%
URJ	109	96.67%	96.77%
URT	98	90%	89.29%
SWGS	93	100%	100%
USCP	102	96.67%	96.43%

- Unbalanced Loads (UL): The UL condition is simulated by positioning weights at the rear of the car.
- Uneven Rail Joint (URJ): To simulate URJ, a piece of tape is applied over the joint area. The red marking indicates the tapes location.
- Uneven Rope Tension (URT): URT is simulated by adjusting the tension of the head springs. The image highlights that the two head springs are more extended compared to the other springs.
- Surface Wear of Guide Shoe (SWGS): The wear of the guide shoe is modeled by altering the distance between the guide shoe and the rail which increases the gap due to wear.
- Uneven Surface in Car Pulley Rope Groove (USCP): The fault in the car pulleys rope groove surface is simulated by affixing tape to simulate unevenness.

B. Accuracy Evaluation

Vibration data from five distinct fault types are used to train the model. The diagnosis performance is then evaluated across these fault categories. To gauge the model's performance, both accuracy and the F1 score are taken into account. The F1 score, which integrates precision and recall into a single metric, is calculated as follows:

$$F1\,Score = 2\frac{(precision * recall)}{(precision + recall)}, \tag{17}$$

where precision refers to the ratio of true positive predictions to the total number of positive predictions, and recall represents the ratio of true positive predictions to the total number of actual positive instances.

Table II summarizes the accuracy verification results for various faults. The SWGS fault shows perfect performance with 100% accuracy and F1 score. The car pulley rope groove surface irregularity achieves 96.67% accuracy and 96.43% F1 score. UL and URJ faults also perform well, with accuracies of 93.33% and 96.67%, and F1 scores of 94.87% and 96.77%, respectively. The URT fault has slightly lower results, with 90% accuracy and 89.29% F1 score. Overall, the model demonstrates strong reliability in fault diagnosis.

C. Feature Extraction Based on Single-axis Data with Triaxial Data

As shown in Fig. 4, extracting features from triaxial vibration data generally produces better results than using single-axis data. This is mainly because different faults cause the elevator to display unique vibration patterns along different axes. Moreover, some faults might not exhibit significant vibration characteristics on a single axis.

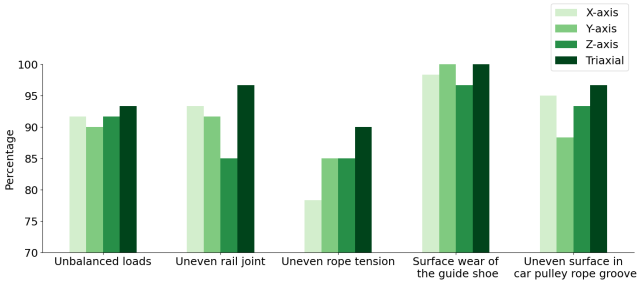

Fig. 4: Feature extraction based on single-axis data and triaxial data.

Elevator vibration characteristics vary by axis depending on the fault type. For example, uneven guideway joints increase front-to-back movement along the X-axis, making X-axis data more effective. Both Y-axis-only and triaxial methods achieve 100% accuracy in diagnosing guide shoe wear, but single-axis data alone reduces performance. Adjusting guide shoe spacing amplifies Y-axis vibrations, ensuring accurate diagnosis with Y-axis data alone.

Faults like unbalanced loads (UL) show different vibrations along the X and Z axes, while others, like uneven rope tension (URT) and surface wear in the car pulley rope groove (USCP), lack distinct single-axis characteristics. Triaxial data improves accuracy by over 2% compared to single-axis data.

Triaxial feature extraction outperforms single-axis methods in both accuracy and reliability, offering a more comprehensive view for improved fault detection.

D. Feature Extraction with and without Elevator Frequency Features

Conventional feature extraction methods overlook the elevator's frequency features.In this experiment, USCP is selected as the test case to compare the proposed method with conventional techniques. As shown in Table III, the conventional approach achieves 93.33% accuracy for diagnosing USCP faults. However, by integrating frequency features, including the car pulleys rotational frequency (Equation (4)), the accuracy increases to 96.67%. These results demonstrate that incorporating frequency features significantly improves fault diagnosis accuracy, outperforming traditional methods.

TABLE III: Result of Frequency Feature Extraction.

Fault	Method	Accuracy	F1 Score
USCP	Before	93.33%	93.10%
	After	**96.67%**	**96.43%**

E. SHAP Features Selection

SHAP orders features based on their values, selecting them in descending order to optimize accuracy while reducing the total number of features. Table IV presents the count of

selected features and the percentage of redundant features removed.

For simple faults like SWGS, distinct vibration patterns allow high accuracy with fewer features. In contrast, more complex faults such as UL and USCP require more features. The multidomain extraction method initially yields 165 features, but SHAP selection removes over 60%, reducing computational load on edge devices. This also improves diagnosis accuracy for faults like UL, URJ, and URT by about 2%, while lowering the risk of overfitting.

TABLE IV: Result of SHAP Features Selection.

Fault	Quantity	Accuracy	Proportion of Redundant Features
UL	**50**	95%	**70%**
URJ	**9**	100%	**95%**
URT	**24**	91.67%	**85%**
SWGS	**1**	100%	**99%**
USCP	**66**	96.67%	**60%**

IV. Conclusion

Existing elevator fault diagnosis methods often overlook the vibration signal characteristics related to mechanical structures and rely on single-axis data, resulting in poor diagnosis outcomes. We propose a multidomain feature extraction method using the structural model of the elevator and triaxial vibration data. This method links abnormal vibrations to specific frequency features, enhancing the model's suitability for fault diagnosis. The key advantage is its ability to integrate vibration information from all directions for a comprehensive fault feature extraction. Experimental results show improved SVM accuracy in diagnosing five types of faults. Additionally, we use SHAP for feature selection to reduce redundant features, decrease computational burden, and minimize the risk of overfitting. Future research could explore deep learning-based feature extraction or real-time fault diagnosis using edge computing to further improve accuracy and practicality. Additionally, integrating multi-sensor data fusion may enhance the system's robustness for complex elevator systems.

References

[1] M. Elnour, A. M. Ahmad, S. Abdelkarim, F. Fodil, and K. Naji, "Empowering smart cities with digital twins of buildings: Applications and implementation considerations of data-driven energy modelling in building management," *Build. Serv. Eng. Res. Technol.*, 2024 MAR 21 2024.

[2] K. Al-Kodmany, "Tall buildings and elevators: A review of recent technological advances," *Buildings*, vol. 5, pp. 1070–1104, SEP 2015.

[3] G. Qing, Q. Zhou, and H. Wang, "Intelligent guidance method for elevator emergency treatment based on automatic recommendation and fault prediction," in *2022 IEEE 22nd International Conference on Software Quality, Reliability, and Security Companion (QRS-C)*, pp. 462–468, IEEE, 2022.

[4] Y. Zhang, Y. Zhao, Z. Yan, S. Feng, and J. Chen, "An image recognition measurement approach and uncertainty for overspeed governors employed in elevator safety," *Build. Serv. Eng. Res. Technol.*, vol. 44, pp. 247–268, MAY 2023.

[5] S.-T. Park and B.-S. Yang, "An implementation of risk-based inspection for elevator maintenance," *J. Mech. Sci. Technol.*, vol. 24, pp. 2367–2376, 2010.

[6] D. Niu, L. Guo, X. Bi, and D. Wen, "Preventive maintenance period decision for elevator parts based on multi-objective optimization method," *J. Build. Eng.*, vol. 44, 2021.

[7] H. Alassafi, K. Al-Gahtani, A. Almohsen, and G. Alfalah, "The causal factors of elevator maintenance: A perspective from saudi arabia healthcare facility management," *Buildings*, vol. 12, MAY 2022.

[8] M. R. Patruni and P. Saraswathi, "Securing internet of things devices by enabling ethereum blockchain using smart contracts," *Build. Serv. Eng. Res. Technol.*, vol. 43, pp. 473–484, JUL 2022.

[9] U. Kumar, S. Mishra, and K. Dash, "An iot and semi-supervised learning-based sensorless technique for panel level solar photovoltaic array fault diagnosis," *IEEE Trans. Instrum. Meas.*, vol. 72, pp. 1–12, 2023.

[10] M. W. Gardner and S. Dorling, "Artificial neural networks (the multilayer perceptron)a review of applications in the atmospheric sciences," *Atmos. Environ.*, vol. 32, no. 14-15, pp. 2627–2636, 1998.

[11] C. Cortes and V. Vapnik, "Support-vector networks," *Mach. Learn.*, vol. 20, pp. 273–297, 1995.

[12] W. Lam and A. M. Segre, "A distributed learning algorithm for bayesian inference networks," *IEEE Trans. Knowl. Data Eng.*, vol. 14, no. 1, pp. 93–105, 2002.

[13] C.-J. Lin and J.-Y. Jhang, "Bearing fault diagnosis using a grad-cam-based convolutional neuro-fuzzy network," *Mathematics*, vol. 9, no. 13, p. 1502, 2021.

[14] M. Jia, X. Gao, H. Li, and H. Pang, "Elevator running fault monitoring method based on vibration signal," *Shock Vib.*, vol. 2021, pp. 1–10, 2021.

[15] K. M. Mishra and K. Huhtala, "Elevator fault detection using profile extraction and deep autoencoder feature extraction for acceleration and magnetic signals," *Appl. Sci.*, vol. 9, no. 15, p. 2990, 2019.

[16] J. Jia, C. Zhang, J. Chen, Z. Zhu, and M. Mao, "Fault diagnosis analysis of angle grinder based on acd-de and svm hybrid algorithm," *Mathematics*, vol. 10, no. 18, p. 3279, 2022.

[17] Z. Wan, S. Yi, K. Li, R. Tao, M. Gou, X. Li, and S. Guo, "Diagnosis of elevator faults with ls-svm based on optimization by k-cv," *J. Electr. Comput. Eng.*, vol. 2015, no. 1, 2015.

[18] Q. Zheng and C. Zhao, "Wavelet packet decomposition and neural network based fault diagnosis for elevator excessive vibration," in *2019 Chinese Automation Congress (CAC)*, pp. 5105–5110, IEEE, 2019.

[19] C. Mo, H. Han, M. Liu, Q. Zhang, T. Yang, and F. Zhang, "Research on svm-based bearing fault diagnosis modeling and multiple swarm genetic algorithm parameter identification method," *Mathematics*, vol. 11, p. 2864, JUL 2023.

[20] P. Wang, B. Xue, J. Liang, and M. Zhang, "Differential evolution with duplication analysis for feature selection in classification," *IEEE Trans. Cybern.*, vol. 53, no. 10, pp. 6676–6689, 2022.

[21] K. Liu, T. Li, X. Yang, H. Chen, J. Wang, and Z. Deng, "Semifree: Semisupervised feature selection with fuzzy relevance and redundancy," *IEEE Trans. Fuzzy Syst.*, vol. 31, no. 10, pp. 3384–3396, 2023.

[22] S. M. Lundberg and S.-I. Lee, "A unified approach to interpreting model predictions," in *Advances in Neural Information Processing Systems 30 (NIPS 2017)* (I. Guyon, U. Luxburg, S. Bengio, H. Wallach, R. Fergus, S. Vishwanathan, and R. Garnett, eds.), vol. 30 of *Advances in Neural Information Processing Systems*, 2017.

[23] J. Hancock, R. Bauder, and T. M. Khoshgoftaar, "A model-agnostic feature selection technique to improve the performance of one-class classifiers," in *2023 IEEE 35th International Conference on Tools with Artificial Intelligence (ICTAI)*, pp. 92–98, IEEE, 2023.

[24] D. Huang, W.-A. Zhang, F. Guo, W. Liu, and X. Shi, "Wavelet packet decomposition-based multiscale cnn for fault diagnosis of wind turbine gearbox," *IEEE Trans. Cybern.*, vol. 53, pp. 443–453, JAN 2023.

[25] E. Strumbelj and I. Kononenko, "An efficient explanation of individual classifications using game theory," *J. Mach. Learn. Res.*, vol. 11, pp. 1–18, 2010.

[26] M. T. Ribeiro, S. Singh, and C. Guestrin, ""why should i trust you?" explaining the predictions of any classifier," in *Proceedings of the 22nd ACM SIGKDD International Conference on Knowledge Discovery and Data Mining*, pp. 1135–1144, 2016.